

Assembly and patterning of the vascular network of the vertebrate hindbrain

Misato Fujita¹, Young R. Cha¹, Van N. Pham¹, Atsuko Sakurai², Beth L. Roman³, J. Silvio Gutkind² and Brant M. Weinstein^{1,4,*}

SUMMARY

The cranial vasculature is essential for the survival and development of the central nervous system and is important in stroke and other brain pathologies. Cranial vessels form in a reproducible and evolutionarily conserved manner, but the process by which these vessels assemble and acquire their stereotypic patterning remains unclear. Here, we examine the stepwise assembly and patterning of the vascular network of the zebrafish hindbrain. The major artery supplying the hindbrain, the basilar artery, runs along the ventral keel of the hindbrain in all vertebrates. We show that this artery forms by a novel process of medial sprouting and migration of endothelial cells from a bilateral pair of primitive veins, the primordial hindbrain channels. Subsequently, a second wave of dorsal sprouting from the primordial hindbrain channels gives rise to angiogenic central arteries that penetrate into and innervate the hindbrain. The chemokine receptor *cxcr4a* is expressed in migrating endothelial cells of the primordial hindbrain channels, whereas its ligand *cxcl12b* is expressed in the hindbrain neural keel immediately adjacent to the assembling basilar artery. Knockdown of either *cxcl12b* or *cxcr4a* results in defects in basilar artery formation, showing that the assembly and patterning of this crucial artery depends on chemokine signaling.

KEY WORDS: Basilar artery, Central arteries, Vasculogenesis, Angiogenesis, Chemokine, Zebrafish

INTRODUCTION

Brain vascular disease has become a topic of intensive study. A thorough knowledge of the developmental biology of cranial vessel formation is important for understanding both development of the central nervous system and cerebrovascular pathologies such as stroke and cerebral hemorrhage. Previous reports have suggested that the primary cranial vasculature is established by vasculogenesis (the assembly of new vessels from the migration and coalescence of mesoderm-derived angioblasts) (Lee et al., 2009). Following the establishment of the primary cranial vessels, a more complex network develops via angiogenesis (the sprouting and growth of new vessels from pre-existing vessels) (Lee et al., 2009). Examination of the vascular anatomy of the developing zebrafish embryo reveals an initial vascular plan that is well conserved compared with that of other developing vertebrates, including humans (Isogai et al., 2001). This conservation extends to the cranial vasculature. The basilar artery (BA) is the first and most important artery to form in the hindbrain. It assembles along the ventral keel of the hindbrain, directly between two primitive bilateral veins known as the primordial hindbrain channels (PHBCs). The BA is one of the most fundamental arteries in the vertebrate head, with many branches irrigating the cerebellum and brainstem. Irrigation of the neural tissues of the hindbrain is accomplished with the help of the slightly later-forming central arteries (CtAs), a set of vessels that penetrate the hindbrain and

interconnect the BA and PHBCs. Like other vertebrates, zebrafish have a BA, PHBCs and CtAs, but the process by which these vessels are assembled and patterned has not been examined in detail in this or any other vertebrate model organism.

The patterning and assembly of other developing vessels have been studied in fish and in other model organisms. Work from a variety of animal models has highlighted the role of extra-endothelial factors as guidance cues that direct the patterning of the developing vasculature, in an analogous manner to the way in which guidance cues direct axon migration and the patterning of the nervous system. The patterning of the trunk vasculature in the zebrafish is directed by a number of different cues. Signaling from midline structures is necessary for primary vascular patterning of the trunk dorsal aorta and cardinal vein (Zhong et al., 2000; Zhong et al., 2001; Lawson et al., 2002; Lawson et al., 2003; Hong et al., 2006; Swift and Weinstein, 2009; Williams et al., 2010), whereas positive and negative somite-derived molecules subsequently regulate the angiogenic growth of trunk intersegmental and parachordal vessels (Torres-Vazquez et al., 2004; Pollard et al., 2006; Wilson et al., 2006; Jones and Li, 2007). These and other recent findings point to the important role of locale-specific patterning mechanisms for blood vessels. Investigating the guidance factors that function during brain vascular network assembly might help to bring a better understanding of the relationship between the development of the vasculature and the central nervous system.

The chemokines, which comprise a group of signaling molecules with important roles in cellular guidance, have recently been implicated in vascular development. Chemokines are vertebrate-specific small (8–14 kDa) proteins that are categorized into four subgroups depending on conserved cysteine residues: C, CC, CXC and CX3C (Viola and Luster, 2008; Raz and Mahabaleshwar, 2009). Chemokines interact with a smaller number of G-protein-coupled seven-transmembrane receptors. Chemokines have been classified into two broad functional categories: inflammatory and

¹Laboratory of Molecular Genetics, Eunice Kennedy Shriver National Institute of Child Health and Human Development, National Institutes of Health, 6B/309, 6 Center Drive, Bethesda, MD 20892, USA. ²Oral and Pharyngeal Cancer Branch, National Institute of Dental and Craniofacial Research, National Institutes of Health, 30/211, 30 Convent Drive, Bethesda, MD 20892, USA. ³Department of Biological Sciences, University of Pittsburgh, Pittsburgh, PA 15260, USA.

*Author for correspondence (bw96w@nih.gov)

homeostatic. The former promote the migration of leukocytes to inflamed tissues, whereas the latter control homeostatic leukocyte trafficking and secondary lymphoid organ structure. Homeostatic chemokines are also involved in a wide variety of developmental migration events, including axon, lateral line, endoderm layer, primordial germ cell, neural crest cell and vascular endothelial cell migration (Olesnicki Killian et al., 2009; Raz and Mahabaleswar, 2009; Siekmann et al., 2009). Mice deficient for chemokine receptor 4 (CXCR4) or its ligand CXCL12 show specific defects in the gut vasculature (Nagasawa et al., 1996; Tachibana et al., 1998). Zebrafish depleted of either *Cxcr4a* or *Cxcl12b* also develop defects in the formation of the anterior lateral dorsal aortae, which form adjacent to the pharynx (Siekmann et al., 2009). Together, these studies suggest a role for chemokine signaling in the fine-tuning of locale-specific vascular patterning.

In this study, we show that the BA forms by a novel combination of angiogenesis-like and vasculogenesis-like processes. BA endothelial cells sprout and migrate from the PHBCs, a pair of pre-existing bilateral primitive veins, in an angiogenesis-like manner. However, after reaching the hindbrain ventral keel, aligned cell clusters gradually lose connections to the PHBCs and the BA assembles entirely from these disconnected cells, without any contribution of cells from other vessels. These latter steps of BA formation are more reminiscent of vasculogenesis. The PHBCs are also the source of the CtA irrigating the hindbrain. CtAs sprout dorsally from the PHBCs, subsequently making connections to the newly formed BA. The zebrafish *cxc4* ortholog *cxc4a* is expressed in PHBC endothelial cells, whereas one of its ligands, *cxc12b*, is expressed in the anterior floor plate in juxtaposition to the assembling BA. Embryos deficient for *cxc12b* and/or *cxc4a* have defects in both BA formation and targeting of CtA connections to the BA. Together, our observations reveal a novel vascular assembly process during hindbrain vascular development, and show that chemokine signaling is involved in guiding the assembly of this vascular network.

MATERIALS AND METHODS

Zebrafish

Zebrafish (*Danio rerio*) embryos were obtained from the natural spawning of laboratory lines. Embryos were raised and fish maintained as described (Kimmel et al., 1995; Westerfield, 2000). Zebrafish lines used were wild-type EK, *Tg(fli1a:EGFP)^{y1}* (Lawson and Weinstein, 2002), *Tg(fli1a:nEGFP)^{y7}* (Roman et al., 2002), *Tg(kdrl:GFP)*, *Tg(gata:DsRed)*, *Tg(pax2a:EGFP)^{el}* (Picker et al., 2002), *Tg(olig2:DsRed2)^{vu19}* (Zannino and Appel, 2009), *Tg(kdrl:mCherry-CAAX)^{y171}* and *Tg(kdrl:nls-mCherry)^{y173}*. For imaging, embryos were either treated with 1-phenyl-2-thiourea (PTU) to inhibit pigment formation (Westerfield, 2000) or *albino* mutant fish were used as reported previously (Kamei and Weinstein, 2005). To immobilize fish for time-lapse imaging they were either treated with tricaine or *chrna1* mutant homozygotes were used (Sepich et al., 1994; Sepich et al., 1998).

Cloning

cxc12b and *cxc4a* cDNA fragments for in situ hybridization were amplified using primers (5' to 3') *cxc12b*-F (ATCCTTGCT-TTGTGGTCCAG) and *cxc12b*-R (TAGCGTTGTGTGACCAGAGG), *cxc4a*-F (ACTTGCTGGAGACTGAAGGAG) and *cxc4a*-R (TGCA-ATGGTCTACATAAGTGC), and cloned into pGEM-T (Promega) and pCRII-TOPO (Invitrogen) vectors, respectively. DIG-labeled antisense riboprobes were synthesized using the DIG Labeling Kit (Roche).

Plasmids containing full-length sequences of *cxc12b* (*cxc12b*/pExpress-1) and *cxc4a* (*cxc4a*/pME18S-FL3) were from Open Biosystems. The full-length sequence of *cxc4a* was cloned into a pCS2+ vector or into a pDestTol2pA2 vector (Kwan et al., 2007; Villefranc et al., 2007) linked with EGFP via a 2A peptide sequence [a viral peptide

sequence that contains an unstable peptide bond, resulting in the stoichiometric co-translational production of two separated proteins (Szymczak et al., 2004)] downstream of the *kdr1* promoter. Capped mRNAs were synthesized using mMessage mMachine Kits (Ambion).

Whole-mount in situ hybridization and immunocytochemistry

RNA in situ hybridization was carried out as previously described (Pham et al., 2007). Antisense mRNA probes for *kdr1*, *cadherin 5*, *dab2*, *flt4* and *dlla4* were prepared as described (Fouquet et al., 1997; Thompson et al., 1998; Lawson et al., 2001; Larson et al., 2004; Siekmann and Lawson, 2007). Immunostaining was performed as described (Matsuda and Chitnis, 2009). Primary antibodies were mouse anti-zebrafish DeltaD (zdd2, Abcam) and rabbit anti-GFP (Invitrogen).

Microscopy

Transmission microscopic imaging of zebrafish embryos was performed using a Zeiss Axioplan 2 compound microscope equipped with a Dage SIT-68 camera. RNA in situ hybridization images were captured with a ProgRes C14 camera mounted on a Leica MZ12 stereomicroscope. Confocal microscopy of transgenic and immunostained embryos was performed using a Radiance 2000 imaging system (Bio-Rad) or a FluoView microscope (Olympus). Time-lapse sequential imaging was performed as described (Kamei and Weinstein, 2005). The images shown in this paper are single-view two-dimensional reconstructions of z-stacks.

Microinjection

Morpholino (Gene Tools; see Table S1 in the supplementary material), DNA and mRNA injection were performed at the described doses into 1- to 2-cell stage embryos.

Chemical treatment of transgenic embryos

Dechorionated *Tg(kdrl:mCherry-CAAX)^{y171}* embryos were treated with either 10 μ M Vegfr2 kinase inhibitor III (SU5416, Calbiochem) or DMSO as a control. As previously reported (Covassin et al., 2006b), SU5416 treatment prior to PHBC assembly results in defects in PHBC formation. Therefore, to specifically examine its effects on BA formation, SU5416 treatment began at 24 hpf, after the PHBCs were fully formed and carrying circulation, to ensure that the cells that normally migrate from the PHBCs to contribute to the BA were all present. Dechorionated *Tg(fli1a:EGFP)^{y1}* embryos were treated with either 30 or 60 μ M PI3K inhibitor (LY294002, Calbiochem) or DMSO control from 24 to 32 hpf.

Blastomere transplantation

Cell transplantation was performed as described (Westerfield, 2000) with the following modifications. Donor *Tg(fli1a:EGFP)^{y1}* embryos were injected at the 1- to 2-cell stage with Cascade Blue-conjugated dextran (D1976, Molecular Probes) as a lineage tracer and with either *cxc4a*-MO2 or control MO. Host *Tg(kdrl:mCherry-CAAX)^{y171}* embryos were injected at the 1- to 2-cell stage with either *cxc4a*-MO2 or control MO. About 20–40 cells were transplanted from donor embryos to the margin of host embryos at sphere stage. The endothelial cell contribution of transplanted cells was assessed by visualization of EGFP expression. Embryos with non-endothelial contribution in the hindbrain area were excluded by visualization of Cascade Blue.

Endothelial cell migration assay

Primary human umbilical vein endothelial cells (HUVECs; C2517A, Lonza) were maintained in the endothelial cell medium EGM-2 BulletKit (CC-3162, Lonza) and then starved overnight before the migration assay. HUVEC migration was evaluated by a modified Boyden chamber assay. SDF-1 α (StemCell Technologies) was diluted to the indicated concentrations in DMEM containing 0.5% BSA. The cells were suspended in DMEM containing 0.5% BSA and 50 μ l (2.5×10^4 cells/well) was loaded into the upper compartment. The cells were pretreated with either 1 μ M *Cxcr4* inhibitor (AMD3100, Sigma), 10 μ M PI3K inhibitor (LY294002, Calbiochem) or no inhibitor for 30 minutes before the migration assay. After incubation for 2.5 or 5 hours at 37°C in 5% CO₂, the cells were fixed in methanol and stained with Eosin and Hematoxylin.

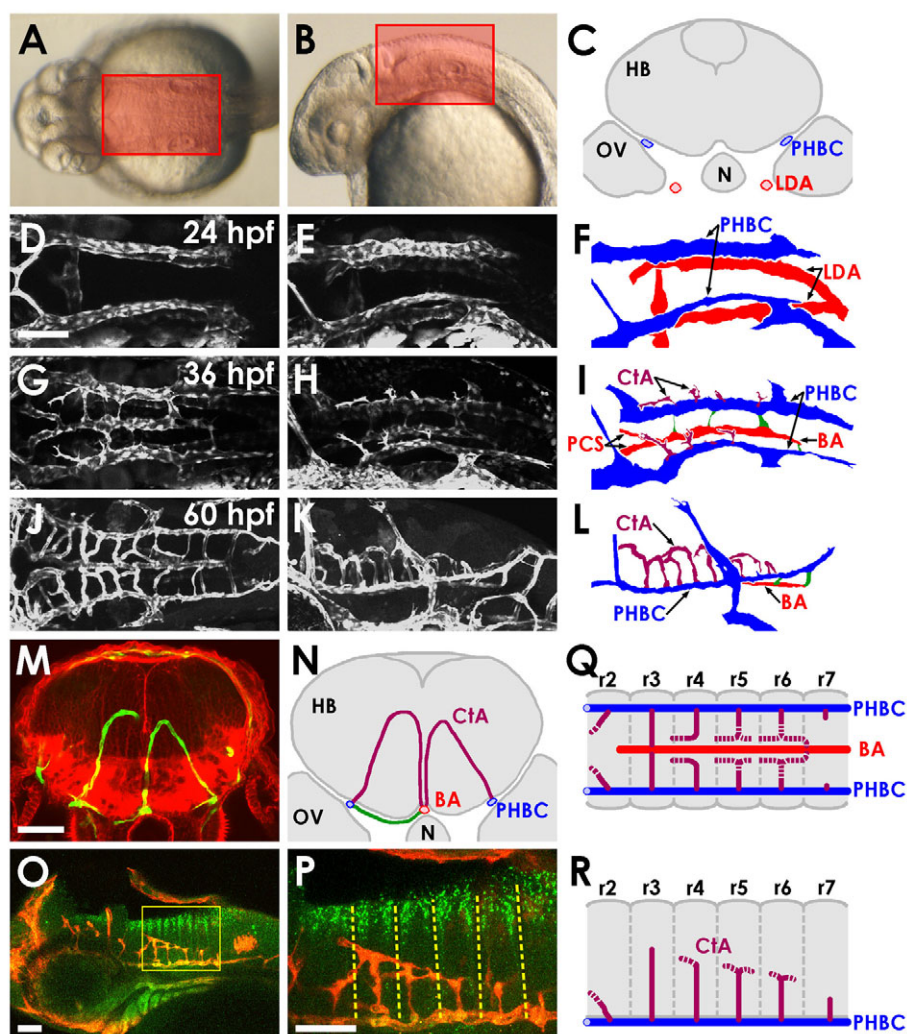


Fig. 1. Vascular anatomy of the developing zebrafish hindbrain. (A,B) Transmitted light images of 30 hpf zebrafish, with boxes indicating the dorsal (A) and lateral (B) regions of the hindbrain imaged here. (C) Schematic transverse section of the hindbrain of a 24 hpf zebrafish, showing the locations of the paired venous primordial hindbrain channels (PHBCs) relative to the hindbrain, otic vesicles, notochord and pharyngeal arterial lateral dorsal aortae (LDA). N, notochord; HB, hindbrain; OV, otic vesicle. (D-L) Confocal images of the hindbrain vasculature in *Tg(fli1a:EGFP)^{Y1}* (D,E,G,H) or *Tg(kdrl:GFP)* (J,K) embryos at 24 (D-F), 36 (G-I) or 60 (J-L) hpf, with explanatory schematic diagrams of the vasculature at each stage (F,I,L). Images and diagrams include dorsal (D,G,J), dorsal-lateral (E,F,H,I) or lateral (K,L) views. Rostral is to the left. Diagrams show LDA (red), PHBC (blue), basilar artery (BA, red) and central arteries (CtAs, purple). (M) Confocal image of a transverse section at the hindbrain level through a 3 dpf *Tg(kdrl:GFP)* embryo (green, blood vessels), counterstained with Rhodamine-phalloidin (red, F-actin). (N) Explanatory diagram of the blood vessels and major anatomical structures in M. Connections (green) persist between the PHBC and BA underneath the hindbrain. (O,P) Whole-mount immunofluorescent staining of blood vessels with anti-GFP (red) and of paraboundary cells with anti-DeltaD (green) in a 60 hpf *Tg(kdrl:GFP)* transgenic embryo. Lateral view, rostral to the left. The boxed area is shown at higher magnification in P. The anti-DeltaD staining efficiently labels rhombomere paraboundary cells, permitting visualization of rhombomere boundaries (dashed lines). (Q,R) Dorsal (Q) and lateral (R) diagrams summarizing the pattern of growth, interconnection and BA linkage of the CtAs. r, rhombomere. Scale bars: 50 μ m.

The cells that migrated to the lower surface of the filters were counted. Eight visual fields were randomly chosen for each assay in order to calculate the average number of migrating cells.

RESULTS

Vascular anatomy of the developing hindbrain

The vasculature of the hindbrain begins as a simple set of vessels, but rapidly develops into a more complex network (Fig. 1A-L). By 24 hours post-fertilization (hpf) a pair of bilateral primitive veins, the PHBCs, come online to either side of the ventral-lateral hindbrain. These vessels form above the lateral dorsal aortae (LDA) and medial to the otic vesicles (Fig. 1C). The LDA are part

of the pharyngeal vasculature, forming serial connections to the developing aortic arches to help supply cranial blood flow, but they are not a part of the brain circulatory system per se. Initially, PHBCs provide the main venous return path for the primitive cranial circulation (Fig. 1D-F). By 36 hpf, a new arterial vessel, the BA, appears below the ventral keel of the hindbrain (Fig. 1G-I). This vessel initially appears as the fused extension of two anterior vessels known as the posterior communicating segments (PCSs) as previously described (Isogai et al., 2001). With continued development, the BA extends further caudally, eventually running along the entire length of the hindbrain. Throughout this stage, direct connections between the PHBCs and the BA are evident on

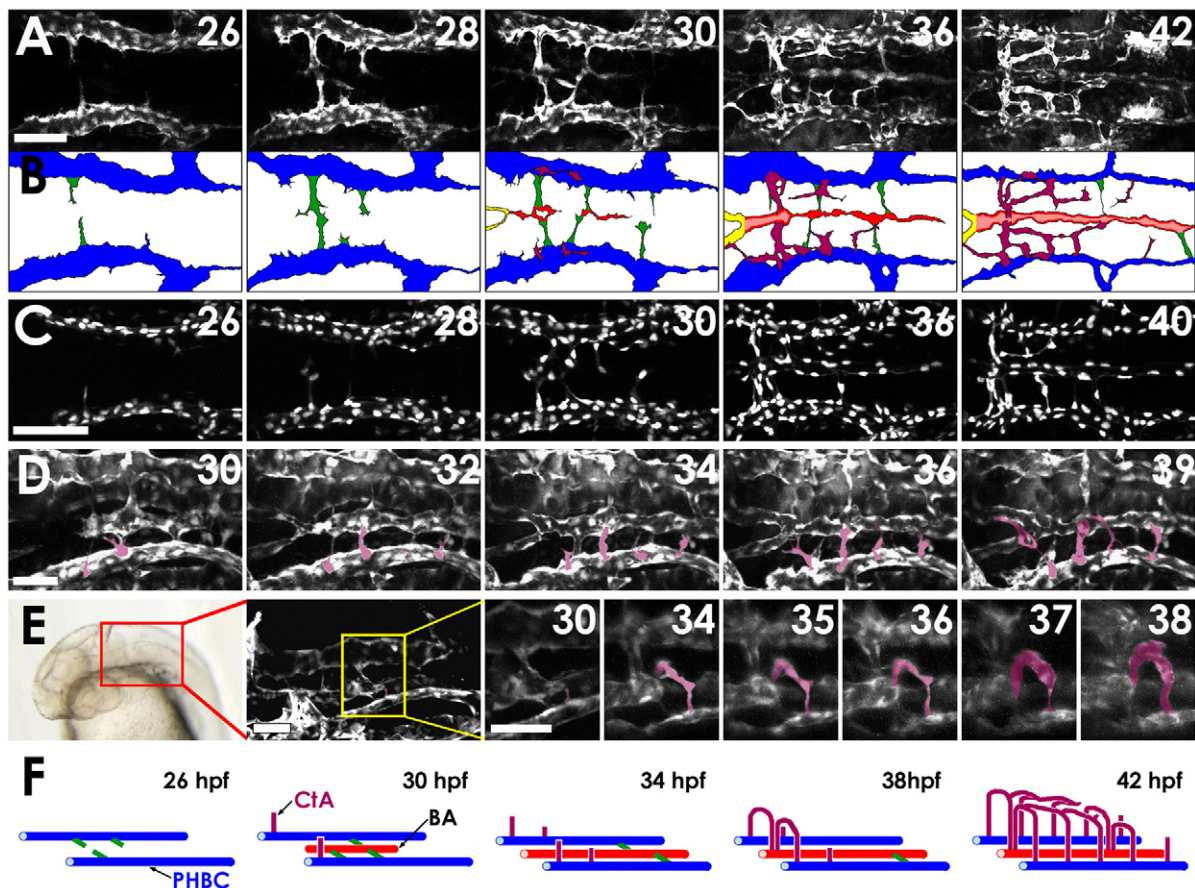


Fig. 2. Two-photon time-lapse imaging of the assembling hindbrain vasculature. (A) Dorsal time-lapse images of BA and CtA formation in the hindbrain of a 26–42 hpf *Tg(fli1a:EGFP)^{y1}* zebrafish embryo (see Movie 1 in the supplementary material). (B) Diagrams of the vessels in A, showing PHBCs (blue), medial sprouts from the PHBCs giving rise to and temporarily connecting to the BA (green), the assembling BA (red), and CtAs sprouting dorsally from the PHBC to form a network connecting to the BA (purple). (C) Dorsal time-lapse images of BA formation in the hindbrain of a 26–40 hpf *Tg(fli1a:nEGFP)^{y7}* embryo (see Movie 2 in the supplementary material). (D) Dorsal-lateral time-lapse images of CtAs sprouting dorsally from the PHBCs in the hindbrain of a 30–39 hpf *Tg(fli1a:EGFP)^{y1}* embryo (see Movie 3 in the supplementary material). CtAs emerging from the left PHBC are pseudocolored purple for ease of visualization. (E) Frontal dorsal-lateral time-lapse images of the r3 CtA (pseudocolored purple for ease of visualization) sprouting dorsally from the PHBCs in the hindbrain of a 30–38 hpf *Tg(kdr1:GFP)* embryo (see Movie 4 in the supplementary material). The red box on the transmitted light image indicates the area visualized in the adjacent confocal image, and the yellow box in that image indicates the area shown at higher magnification in the remaining panels, which includes the r3 CtA. (F) Model of hindbrain vascular development (color scheme as in B). Scale bars: 50 μ m in A,C; 25 μ m in D,E.

the ventral surface of the hindbrain, but these early ventral connections all disappear at later stages (Fig. 1G,I and see Fig. S1 in the supplementary material).

By 60 hpf, a new network of dorsally projecting vessels, the CtAs, has formed to interconnect the PHBCs and BA (Fig. 1J–L). Unlike the BA and PHBCs, which are adjacent to, but outside of, the hindbrain, these arch-shaped vessels penetrate up into the hindbrain tissue itself (Fig. 1M,N). The most rostral set of CtAs connects the PCSs (Fig. 1I) and PHBCs on either side, whereas the more caudal CtAs all connect the BA and PHBCs. The CtAs exhibit a regular pattern of projection from the PHBCs that is reminiscent of the metamerically repeating pattern of the trunk intersegmental vessels (ISVs). The trunk and the hindbrain are both divided into repeating anatomical units: somites in the trunk, rhombomeres for the hindbrain. The ISVs run along intersomitic boundaries. Whole-mount double immunostaining of 60 hpf *Tg(fli1a:EGFP)^{y1}* embryos using an anti-DeltaD antibody (Matsuda and Chitnis, 2009) to label rhombomere paraboundaries and an anti-GFP antibody to label blood vessels revealed that a CtA

projects through the center of each rhombomere, but not along the boundaries (Fig. 1O,P). We confirmed this by examining *Tg(kdr1:mCherry-CAAX)^{y171}*; *Tg(pax2a:GFP)^{e1}* double-transgenic zebrafish embryos, which express membrane-localized mCherry in blood vessels and GFP in the third and fifth rhombomeres (see Fig. S2 in the supplementary material). CtAs were detected initially through the center of the third rhombomere (r3), then through the center of other rhombomeres slightly later. As noted above, the most rostral (r2) CtAs connect to the two PCSs, whereas more caudal CtAs (r3 through r7) connect to the BA (Fig. 1Q,R).

Assembly of the hindbrain vasculature

We performed time-lapse imaging using *Tg(fli1a:EGFP)^{y1}*, *Tg(fli1a:nEGFP)^{y7}* or *Tg(kdr1:GFP)* embryos to examine how the BA and CtAs assemble (Fig. 2A–F and see Movies 1–4 in the supplementary material). The bilateral PHBCs (blue in Fig. 2B) come on line by 22 hpf, assembling by vasculogenesis from angioblasts migrating from rostral and caudal mesodermal precursors. By 26 hpf, vascular sprouts (green) begin to emerge

from the medial walls of the PHBCs and grow towards the midline (Fig. 2A,B and see Movie 1 in the supplementary material). By 28 hpf, the sprouts from either side start to meet at the midline, and by 30 hpf the endothelial cells that have reached the midline start to align longitudinally and extend further caudalward (red), beginning BA formation. By 36 hpf, the rostral tip of the BA connects with the two PCSs (yellow) and the BA becomes lumenized and starts to carry circulation. As noted above, the initial connections to the PHBCs (green) start to be lost once the BA has assembled, with the peak number of ventral connections to the PHBCs found at approximately 33 hpf (see Fig. S1 in the supplementary material). A few of these ventral connections persist for some time, providing early venous drainage for the BA, although these also disappear at later stages (Isogai et al., 2001). We examined the cellular contribution to the BA by performing time-lapse imaging using *Tg(fli1a:nEGFP)^{y7}* transgenic embryos, which express a nuclear-targeted EGFP in endothelial cells permitting tracing of the migration and division of individual endothelial cell nuclei (Fig. 2C and see Movie 2 in the supplementary material). These experiments confirmed that the endothelial cells forming the BA all migrate from the PHBCs, losing their connections to the PHBCs once assembly of the BA is complete.

CtA sprouts emerge from the dorsal walls of the PHBCs by 30 hpf (Fig. 2A,D and see Movies 1 and 3 in the supplementary material). The first sprouts usually appear in r3, with more caudal CtA sprouts appearing sequentially thereafter. The sprouts grow dorsally through the center of each rhombomere, then turn medially after having traveled approximately two-thirds dorsally through the rhombomere. CtA sprouts do not cross the midline. The r3 CtA then turns ventrally and connects to the BA (Fig. 2E and see Movie 4 in the supplementary material). Other CtAs also connect to the BA at slightly later stages (Fig. 3A,B), after first anastomosing with r3 and other CtAs at their dorsal-most point (Fig. 1Q and see Movie 1 in the supplementary material). CtAs are generated entirely by sprouting and growth from the PHBCs, with eventual connection to the BA; no sprouts emerge from the BA. Interestingly, growing CtAs appeared to avoid oligodendrocyte progenitor cells and abducens motor neuron precursors in the medial ventral area of r5 and r6, suggesting that these neuronal clusters might provide negative cues for CtA growth (Fig. 3C,D).

In order to examine whether circulatory flow plays a role in the assembly and patterning of either the BA or the CtA, we injected morpholino antisense oligonucleotide (MO) that targets *cardiac troponin T2a* (*tnnt2a*) mRNA into *Tg(fli1a:EGFP)^{y1}* zebrafish embryos. Embryos deficient in *tnnt2a* have a nonfunctional 'silent heart' and are routinely used for assessment of the role of circulatory flow in the development of other tissues (Sehnert et al., 2002). We found that the patterning of the BA and CtAs was not significantly altered by lack of circulatory flow, although most vessels appeared thinner, probably owing to a lack of intravascular pressure and/or defects in lumenization (Fig. 3E-H).

Taken together, our results indicate that the BA is formed by medialward sprouting and migration of endothelial cells from pre-existing veins – the PHBCs. Once migration is complete, BA endothelial cells become disconnected from their source and the BA develops as a completely separate artery. The formation of the BA thus bears resemblance to both angiogenesis (sprouting from pre-existing vessels) and vasculogenesis (formation of new vessels by coalescence of migratory angioblast progenitors). By contrast, the CtAs appear to develop exclusively via sprouting angiogenesis, with all sprouts emerging from the PHBCs dorsally.

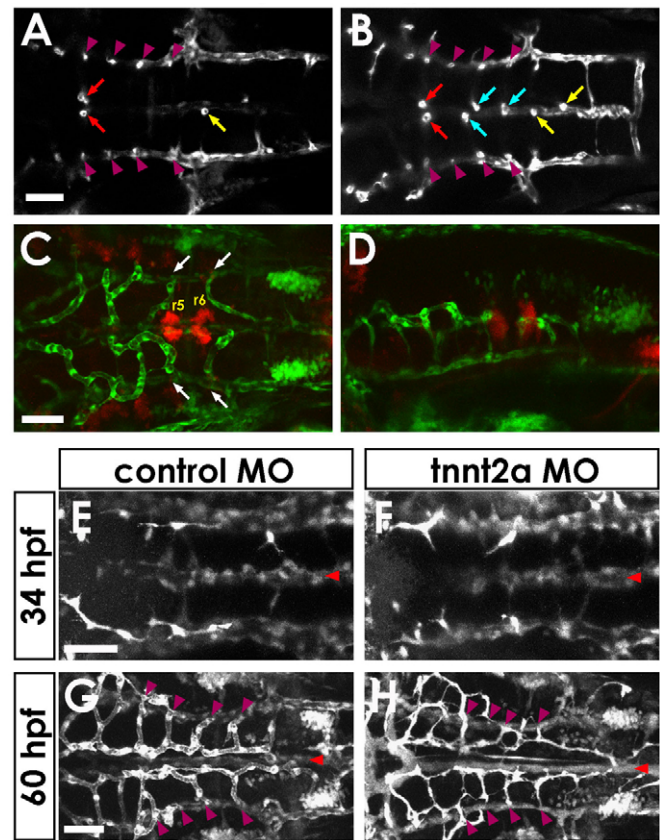


Fig. 3. Central artery formation and patterning. (A,B) Single horizontal section through the hindbrains of 54 (A) and 60 (B) hpf *Tg(kdrl:GFP)* embryos. The CtA in the third rhombomere (r3) links directly to the BA from early stages (red arrows in A), whereas CtAs in r4 and r5 do not initially connect to the BA. One or two direct connections are also usually present in r6 or r7 (yellow arrow in A) by this stage. Direct connections in r4 and r5 are formed later (blue arrows in B). Each stem of the CtAs in r3 to r6 is indicated by a purple arrowhead. (C,D) CtAs avoid *Olig2⁺* clusters in r5 and r6. Dorsal (C) and lateral (D) view of confocal images in a 48 hpf *Tg(fli1a:EGFP)^{y1}; Tg(olig2:DsRed2)^{vu19}* double-transgenic embryo, showing *DsRed2*-positive neuroepithelial precursors (red) and EGFP-positive blood vessels (green). The CtAs in r5 and r6 (arrows) appear to turn away from and avoid the nearby *Olig2⁺* clusters. (E-H) CtAs are patterned normally in *tnnt2a* MO-injected 'silent heart' animals that lack blood circulation. Confocal images of the hindbrain vasculature in 34 (E,F) and 60 (G,H) hpf *Tg(fli1a:EGFP)^{y1}* control (E,G) or *tnnt2a* (F,H) MO-injected zebrafish embryos. BA, red arrowheads; CtAs, purple arrowheads. Dorsal view, rostral to the left. Scale bars: 50 μ m.

Acquisition of arterial identity during basilar artery formation

We examined the staged expression of markers of arterial or venous endothelial identity using RNA in situ hybridization to study the acquisition of arterial identity during BA formation. The pan-endothelial markers *kdrl* and *cadherin 5* were expressed throughout the cranial vasculature, including the PHBCs, BA and LDAs (see Fig. S3A-H in the supplementary material). The PHBC has a venous molecular identity and expressed the venous molecular markers *flt4* and *dab2* at 1 day post-fertilization (dpf) (see Fig. S3I-P in the supplementary material) (Bussmann et al., 2007; Jin et al., 2007). *flt4* expression was detected in the PHBCs during BA formation, but was absent from the BA and other arteries such as

the LDA. *dab2* was weakly expressed in the LDAs (see Fig. S3M,N in the supplementary material) but much more strongly expressed in the PHBCs (see Fig. S3O in the supplementary material). Interestingly, *dab2* expression was reduced in central and caudal portions of the PHBCs at 32 hpf, during BA formation (see Fig. S3P in the supplementary material). At the same time, the arterial marker *dll4* (Leslie et al., 2007) was expressed in the cranial arteries, including the LDAs (see Fig. S3S in the supplementary material) and began to be expressed in some cells in the central PHBCs as well as in the newly forming BA (see Fig. S3R,T in the supplementary material). These expression patterns suggest that some endothelial cells in the PHBCs lose their venous identity and acquire arterial and/or tip cell identity before migrating to form the BA.

VEGF signaling is required for basilar artery formation

VEGF signaling has been exhaustively demonstrated as absolutely required for vessel formation during both vasculogenesis and angiogenesis in multiple models. Zebrafish cranial vessel formation is not an exception. Embryos injected with MOs targeting *vegfc* or *flt4* have defects in PHBC formation (Covassin et al., 2006a). Combined loss of *flt4* (*vegfr3*) and *kdr1* (*kdra*), one of two *vegfr2* orthologs in zebrafish, exacerbates this phenotype, and treatment with the VEGF signaling inhibitor SU5416 prevents PHBC formation (Covassin et al., 2006a). Embryos lacking three Vegf receptors [Kdr1, Kdr (Kdrb) and Flt4] show the most severe lack of cranial veins (Covassin et al., 2006a).

Since PHBC defects would secondarily affect later BA formation, we treated embryos with SU5416 from 24 to 30 hpf, after the PHBCs have assembled, to attempt to identify the functional requirement for VEGF signaling during BA formation from PHBC-derived endothelial progenitors. We found that the formation of both BA and CtAs was abolished in SU5416-treated embryos (see Fig. S4 in the supplementary material). These results indicate that VEGF signaling at later stages is also required for BA and CtA formation, although reduced enlargement of the PHBC by endothelial proliferation was also noted in 24–30 hpf SU5416-treated animals (see Fig. S4 in the supplementary material).

Chemokine signaling is required for hindbrain vascular patterning

To explore the molecular cues directing hindbrain vascular patterning, we examined a variety of genes implicated in guidance processes to see whether the spatial and temporal expression patterns of any of these genes would suggest a potential role in guiding the formation of either the BA or CtA. During the stages of BA formation, the chemokine ligand *cxcl12b* is expressed in the anterior floor plate and its putative receptor *cxcr4a* is expressed in the PHBCs. Hindbrain floor plate expression of *cxcl12b* was strong at 32 hpf as the BA is assembling at the midline, but was absent at 24 hpf and weaker at 52 hpf (Fig. 4A–F). In addition to floor plate expression (arrows in Fig. 4B,E and see Fig. S5A,C in the supplementary material), *cxcl12b* was also expressed in the pharyngeal endoderm just ventrolateral to the LDA (arrowheads in Fig. 4A,D and see Fig. S5A,C in the supplementary material). As previously reported (Siekman et al., 2009), pharyngeal endoderm provides a ‘track’ that links together rostral and caudal portions of the developing LDA. *cxcr4a* is expressed in cranial endothelial cells (Fig. 4G–L). At 24 hpf, *cxcr4a* expression was detected in the LDAs (arrowheads in Fig. 4G,J) and pharyngeal arches (arrows in Fig. 4G,J) in the ventral pharynx area (Olesnick Killian et al.,

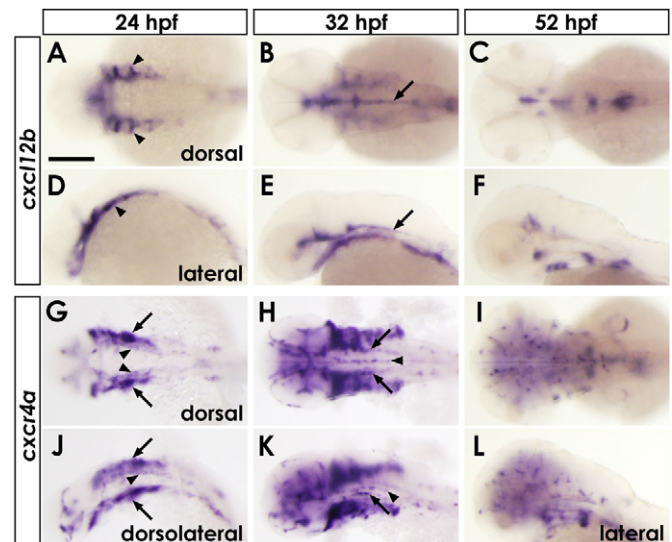


Fig. 4. Expression patterns of *cxcl12b* and *cxcr4a*. (A–L) Whole-mount in situ hybridization of 24 (A,D,G,J), 32 (B,E,H,K) and 52 (C,F,I,L) hpf wild-type zebrafish embryos, probed for either *cxcl12b* (A–F) or *cxcr4a* (G–L). Dorsal (A–C,G–I), lateral (D–F,L) and dorsolateral (J,K) views are shown, with rostral to the left. Arrowheads in A,D, pharyngeal endoderm; arrows in B,E, anterior floor plate; arrowheads in G,J, LDA; arrows in G,J, pharyngeal arches; arrowheads in H,K, BA; arrows in H,K, PHBC. For detailed expression patterns in transverse sections, see Fig. S5 in the supplementary material. Scale bar: 200 μ m.

2009; Siekman et al., 2009). Soon after, *cxcr4a* began to be expressed in the PHBCs (arrows in Fig. 4H,K and see Fig. S5B,D in the supplementary material) and newly forming BA (arrowheads in Fig. 4H,K and see Fig. S5B,D in the supplementary material) in the hindbrain. At 52 hpf and later stages, punctate expression of *cxcr4a* was observed throughout the head (Fig. 4I,L). Together, the expression data show that during BA assembly, *cxcl12b* is expressed in the ventral midline of the hindbrain, whereas its receptor *cxcr4a* is expressed in the newly forming BA and in the PHBCs from which BA progenitors emerge, suggesting that Cxcl12b-Cxcr4a signaling might play a role in BA formation.

To determine whether Cxcl12b-Cxcr4a chemokine signaling is required for BA formation, we utilized MOs to knock down Cxcl12b and/or Cxcr4a in *Tg(fli1a:EGFP)^{y1}* animals. We used *cxcl12b* and *cxcr4a* MOs (*cxcl12b*-MO1, *cxcr4a*-MO1) previously shown to be effective in knocking down their respective gene products (Knaut et al., 2003; Siekman et al., 2009). We also verified our results using two additional MOs against each gene (*cxcl12b*-MO2, *cxcr4a*-MO2), which yielded essentially indistinguishable phenotypes. Embryos injected with *cxcl12b*-MO2, *cxcr4a*-MO2, or both MOs together at half doses of each (‘double MO’), appeared morphologically normal compared with their control MO-injected siblings (Fig. 5A,D,G,J). A previous report (Siekman et al., 2009) demonstrated that embryos mutated for *cxcr4a* or injected with a *cxcl12b* or *cxcr4a* MO develop comparable defects in anterior LDA formation. In agreement with this previous report, we observed analogous defects in LDA formation upon *cxcl12b*-MO2, *cxcr4a*-MO2, or double MO injections, verifying the efficacy of our MOs and confirming that Cxcl12b-Cxcr4a signaling is crucial for proper LDA formation (see Fig. S6 in the supplementary material).

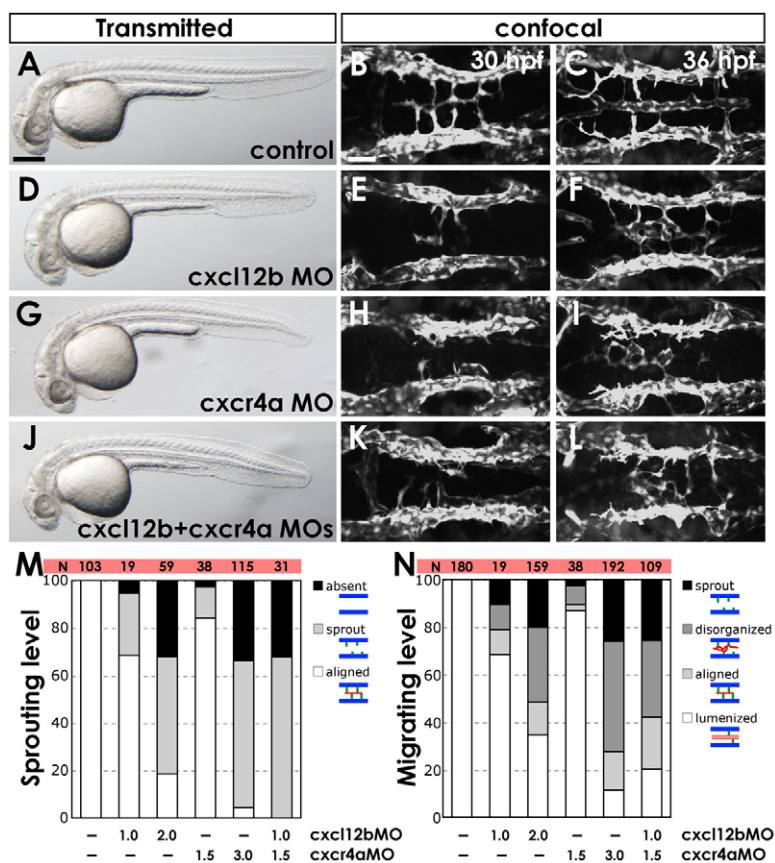


Fig. 5. Chemokine signaling is required for hindbrain vascular patterning. (A-L) BA assembly defects are present in *cxc4a* MO- and *cxc12b* MO-injected *Tg(fli1a:EGFP)^{y1}* zebrafish embryos. (A,D,G,J) Transmitted light images of 32 hpf animals; lateral view, rostral to the left. (B,C,E,F,H,I,K,L) Confocal images of the hindbrain vasculature in 30 (B,E,H,K) or 36 (C,F,I,L) hpf animals; dorsal view, rostral to the left. Animals were injected with control MO (A-C), 2 ng *cxc12b*-MO2 (D-F), 3 ng *cxc4a*-MO2 (G-I), or 1 ng *cxc12b*-MO2 + 1.5 ng *cxc4a*-MO2 (J-L). (M) The percentage of 30 hpf MO-injected animals with no PHBC sprouts ('absent'), PHBC sprouts that do not extend to or align along the midline ('sprout'), or BA endothelial cells aligned along the ventral keel of the hindbrain ('aligned', which is normal for this stage). (N) The percentage of 36 hpf MO-injected animals with PHBC sprouts that do not extend to or align along the midline ('sprout'), BA endothelial cells near the midline but not aligned longitudinally ('disorganized'), endothelial cells aligned along the ventral keel of the hindbrain but not lumenized ('aligned'), or with an assembled, lumenized BA ('lumenized', which is normal for this stage). For illustration of phenotypic categories, see Fig. S7 in the supplementary material. Scale bars: 250 μ m in A; 50 μ m in B.

Formation of the PHBC and trunk blood vessels was normal at 24 hpf in each morphant, but defects in BA formation became evident by 30 hpf (Fig. 5B,E,H,K,M and see Fig. S7A in the supplementary material). The emergence, medial migration and midline alignment of sprouts from the PHBCs were impaired at 30 hpf in animals injected with full doses of *cxc12b*-MO2 or *cxc4a*-MO2, or double MO. By 36 hpf, sprouts emerged from the PHBCs in most morphants, but the majority of these sprouts failed to migrate to the midline, align or form a lumenized BA (Fig. 5C,F,I,L,N and see Fig. S7B in the supplementary material). The MO phenotypes were dose dependent, with strong synergy in double MO-injected animals (Fig. 5M,N). In addition to failing to assemble the BA, PHBC sprouts in *cxc4a* MO-injected and/or *cxc12b* MO-injected animals were often misdirected, with abnormal connections to the incomplete LDA (Fig. 6 and see Movies 5 and 6 in the supplementary material). Our observations at these two different time points suggest that Cxcl12b-Cxcr4a chemokine signaling functions for both the induction of BA sprouts and their guidance to the midline.

Defects in CtA formation were also noted in animals injected with *cxc12b* MO, *cxc4a* MO or double MO. CtAs sprouted normally from the dorsal aspect of the PHBCs at 30 hpf, but the sprouts failed to reach the BA at 42 hpf, when the CtAs in r3 should become connected to the BA. However, it is not clear whether the defects in CtA targeting to the ventral midline reflect a direct requirement for midline chemokine signaling or a failure to properly form the ultimate target for CtA connection, the BA. To examine the correlation, MO-injected animals were scored and grouped by their BA phenotype at 36 hpf (sprout, disorganized, aligned, lumenized) and then rescored at 42 hpf for r3 CtA phenotypes (link in r3, midward, or dorsalward). We found that the

groups of animals with stronger BA phenotypes were also those with more dramatic r3 CtA phenotypes (see Fig. S8 in the supplementary material).

We performed mRNA rescue experiments to verify that the vascular defects in *cxc4a* MO-injected animals reflect a genuine functional requirement for chemokine signaling. We injected *cxc4a*-MO2 into *Tg(fli1a:EGFP)^{y1}* animals with or without co-injection of wild-type *cxc4a* mRNA and assessed medial-lateral sprouting of the PHBC at 30 hpf. PHBC sprouting was almost completely rescued in mRNA-injected animals, compared with only ~55% sprouting in sibling animals injected with *cxc4a*-MO2 alone (Fig. 7A).

We also carried out additional experiments to verify that the BA defects in *cxc4a* MO-injected animals reflect an endothelial cell-autonomous requirement for chemokine signaling. We co-injected *cxc4a*-MO2 into *Tg(kdrl:mCherry-CAAX)^{y171}* or *Tg(kdrl:nls-mCherry)^{y173}* embryos together with a *kdr:egfp-2A-cxc4a* transgene or a control *kdr:egfp* transgene, and measured the number of transgene-expressing endothelial cells migrating medially from the PHBCs (Fig. 7B-E). The percentage of transgene-expressing medially migrating endothelial cells was increased in *kdr:egfp-2A-cxc4a* transgene-injected animals as compared with control *kdr:egfp* transgene-injected animals, demonstrating that endothelial-autonomous restoration of Cxcr4a function is sufficient to promote medial migration of PHBC endothelial cells in *cxc4a* morphants (Fig. 7F). We also performed blastomere transplantation experiments to further verify the endothelial cell-autonomous requirement for chemokine signaling during BA migration (Fig. 7G-K). Donor *Tg(fli1a:EGFP)^{y1}* embryos (to mark donor-derived endothelial cells) were co-injected with either *cxc4a*-MO2 or control MO plus Cascade Blue-conjugated dextran (to mark all donor-derived cells).

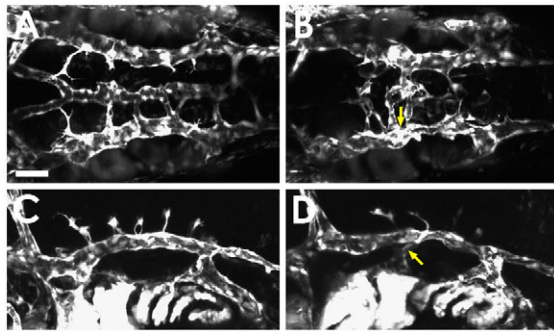


Fig. 6. Abnormal connections between the lateral dorsal aortae and posterior hindbrain channels in *cxc4a* morphants.

(A–D) Example of a misdirected vessel in *cxc4a* MO-injected zebrafish. Confocal images of the hindbrain vasculature in 36 hpf control (A,C) and *cxc4a* (B,D) MO-injected *Tg(fli1a:EGFP)^{y1}* animals. Dorsal (A,B) and lateral (C,D) views. Abnormal connections between the LDA and PHBC are occasionally observed in *cxc4a* morphants (yellow arrows), but are never found in control MO-injected animals. The confocal image stacks used to generate these images are shown in Movies 5 and 6 in the supplementary material. Scale bar: 50 μ m.

Host *Tg(kdrl:mCherry-CAAX)^{y171}* embryos (to mark host endothelial cells), were injected with either *cxc4a*-MO2 or control MO. The percentage of transplanted medially migrating PHBC endothelial cells was increased when the cells were derived from a wild-type donor, irrespective of whether the host embryo was *Cxcr4a* positive (Fig. 7K).

It has been reported that the migration of endothelial progenitor cells is mediated by CXCR4 via the PI3K/Akt/eNOS signal transduction pathway (Zheng et al., 2007). To examine the migration behavior and PI3K requirement of differentiated endothelial cells in response to CXCL12 stimulation, we performed a migration assay using human umbilical vein endothelial cells (HUVECs), which are known to express CXCR4 (Volin et al., 1998). Human recombinant SDF-1 α (CXCL12) induced HUVEC migration in a dose-dependent manner (see Fig. S9A in the supplementary material). SDF-1 α -induced migration was inhibited by treatment with the CXCR4-specific peptide antagonist AMD3100 or the PI3K inhibitor LY294002, indicating that SDF-1 α -induced endothelial migration is promoted specifically via its receptor CXCR4 through the PI3K signaling pathway (see Fig. S9B in the supplementary material). To evaluate the functional role of PI3K in vivo during BA migration, *Tg(fli1a:EGFP)^{y1}* zebrafish embryos were treated with LY294002 from 24 to 32 hpf. BA migration was arrested in LY294002-treated embryos (see Fig. S9C,D in the supplementary material). Taken together, these results demonstrate that the PI3K signal transduction pathway plays an important role as a downstream component in both SDF-1 α -induced HUVEC migration and Cxcl12-Cxcr4-induced BA assembly.

DISCUSSION

In this study, we examined the assembly and patterning of the vascular network of the vertebrate hindbrain. A related study in this same issue also examines the mechanisms of hindbrain vascular development using the zebrafish (Bussmann et al., 2011). We have previously described the vascular anatomy of the developing zebrafish by microangiography, a method that permits visualization of patent vessels connected to the circulation, but not vessels in the

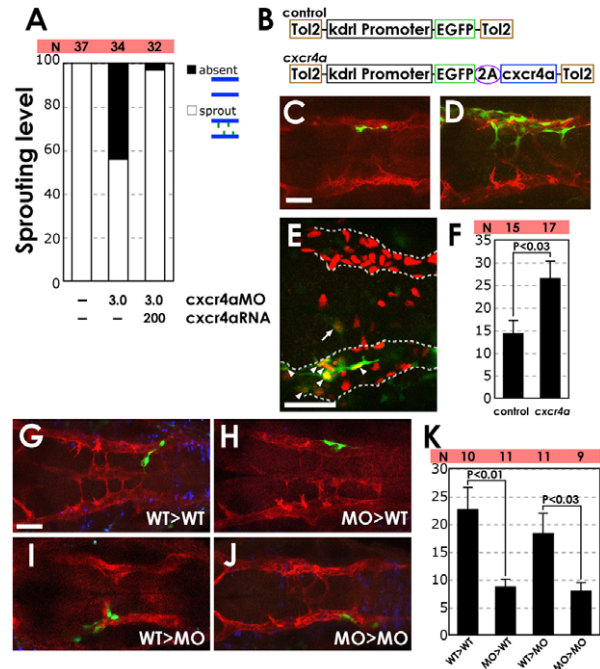


Fig. 7. Expression of *cxc4a* promotes PHBC sprouting and medial migration in *cxc4a* MO-injected animals. (A) Co-injection of 200 pg mRNA encoding wild-type *cxc4a* alleviates the PHBC sprouting defect in zebrafish injected with 3 ng *cxc4a*-MO2. The percentage of 30 hpf *Tg(fli1a:EGFP)^{y1}* animals showing endothelial cells migrating medially from the PHBC. The number of embryos analyzed for each injection is shown (N). (B) The Tol2 transposon cassettes of the control (*kdrl:egfp*) and *cxc4a* (*kdrl:egfp-2A-cxc4a*) expression vectors; the latter includes the 2A peptide sequence (see Materials and methods). (C, D) Confocal images of the hindbrain vasculature in 36 hpf *cxc4a*-MO2-injected *Tg(kdrl:mCherry-CAAX)^{y171}* embryos co-injected with either control *egfp* transgene (C) or with a *cxc4a* and *egfp* co-expression transgene (D). Dorsal view, rostral to the left. (E) Sample confocal image of the hindbrain vasculature in a 36 hpf *Tg(kdrl:nls-mCherry)^{y173}* embryo (with red fluorescent endothelial nuclei) injected with *cxc4a*-MO2 and control *kdrl:egfp* transgene (green fluorescent endothelial cell bodies). In this animal, one EGFP-expressing endothelial cell (arrow) has migrated medially from the PHBC, whereas six EGFP-expressing endothelial cells (arrowheads) are present within the PHBC (outlined by a dashed line). Dorsal view, rostral to the left. (F) Quantification (percentage) of the medial migration tendency of transgene-expressing cells. The number of medially migrating EGFP-expressing endothelial cells (one in the example E) out of the total number of EGFP-expressing hindbrain endothelial cells (seven in the example E) was determined in 15 control (*kdrl:egfp*) and 17 *cxc4a* (*kdrl:egfp-2A-cxc4a*) animals. The s.e.m. is 2.9 for the control group and 3.9 for the *cxc4a* group. The variability range of the two groups was comparable ($P > 0.1$, F-test), and a *t*-test shows that the two groups are statistically different ($P < 0.03$). (G–J) Confocal images of the hindbrain vasculature in *Tg(kdrl:mCherry-CAAX)^{y171}* transgenic host embryos from either wild type (WT) to WT (control MO-injected donor to control MO-injected host) (G), MO to WT (*cxc4a*-MO2-injected donor to control MO-injected host) (H), WT to MO (I) or MO to MO (J) transplants. Dorsal view, rostral to the left. Transplanted cells were labeled with Dextran Blue. Transplanted vascular endothelial cells also express EGFP because *Tg(fli1a:EGFP)^{y1}* embryos were used as donors. (K) Quantification (percentage) of the medial migration tendency of transplanted cells. The number of medially migrating EGFP-expressing endothelial cells out of the total number of EGFP-expressing hindbrain endothelial cells was determined in ten (WT to WT), 11 (MO to WT), 11 (WT to MO) and nine (MO to MO) injected animals. Average percentages of medially migrated transplanted endothelial cells and s.e.m. were calculated for all groups. Scale bars: 50 μ m.

process of assembling (Isogai et al., 2001). The primitive hindbrain vasculature consists of two bilateral longitudinal veins running ventral-lateral to the hindbrain and medial to the otic capsule (the PHBCs), a single medial longitudinal artery at the ventral keel of the hindbrain (the BA), and a network of dorsally projecting smaller vessels that penetrate the hindbrain proper and interconnect the three primary ventral vessels (the CtAs). The PHBCs are formed during primary vasculogenesis from mesoderm-derived angioblasts. In this report, we show that the BA assembles by a novel hybrid vasculogenesis/angiogenesis process from endothelial cells that emerge in an initial wave of medialward sprouting from the PHBCs. We further show that the CtAs develop exclusively via sprouting angiogenesis, also from the PHBCs, in a second wave of dorsalward sprouting. The CtAs form in a metamerically repeating pattern with a single CtA projecting upward through the center of each rhombomere on either side of the hindbrain. Our results demonstrate that, like the trunk vasculature, the hindbrain vasculature forms in a stereotyped, stepwise fashion.

The PHBCs serve as the main routes for venous drainage from the head from the initiation of cranial circulation at approximately 1 dpf until approximately 2.5 dpf, when the primary head sinuses (PHS) take the place of the PHBCs (Isogai et al., 2001). Our time-lapse imaging results show clearly that the PHBCs are the only source of endothelial cells populating the BA. Recent genetic studies support the venous identity of the PHBCs, showing that these vessels express known venous molecular markers, such as *flt4* and *dab2* (Bussmann et al., 2007; Jin et al., 2007). Our observations reveal that endothelial cells in certain portions of the PHBC lose venous identity and adopt arterial and/or tip cell identity during BA formation, indicating that the PHBC acquires mixed arterial-venous character. Classical anatomical studies suggest that the BA in humans is derived from paired arterial vessels termed the bilateral longitudinal neural arteries [LNAs (Padget, 1956)]. The paired LNAs are located at the medial edge of two bilateral vascular plexuses, the lateral edges of which form the PHBCs. The medial edges of the LNAs migrate to the midline and undergo ‘zippering together’ to form a single midline BA. The lateral edges of the LNA gradually detach most venous connections from the PHBC, a transient structure that is almost immediately superseded in function by the PHS. Thus, the resolution of the vascular plexus containing the PHBC and LNA to form the BA in humans has strong parallels to BA development from the PHBC in zebrafish, although zebrafish embryos do not form a plexus during BA assembly.

The differences and similarities between BA formation in the human and zebrafish hindbrain are also reminiscent of the differences in trunk dorsal aorta assembly between zebrafish, mammals and avians. During zebrafish development, the dorsal aorta forms from lateral mesodermal angioblasts that migrate medially and assemble into a single midline vascular tube. In mammals and avians, paired lateral dorsal aortae assemble at the medial edge of the bilateral primitive venous plexuses, subsequently merging together medially to form a single midline aorta and losing most venous connections (Coffin and Poole, 1988; Coffin et al., 1991; DeRuiter et al., 1993). As noted previously (Isogai et al., 2001), many vessel assembly processes seem ‘accelerated’ in the fish compared with mammals, with some intermediate stages of vascular development in mammals, such as plexus formation or the appearance of bilateral paired BAs or dorsal aortae, skipped over in the fish. There are other similarities and some notable differences between the formation of the hindbrain vascular network described here and the process of trunk vascular network assembly that we reported on previously (Isogai

et al., 2003). As in the trunk vasculature, two successive waves of vascular sprouting occur in the hindbrain during vascular network assembly. In the trunk these comprise the primary and secondary ISVs; in the hindbrain these generate the BA and CtAs. In the case of the trunk, the two waves of sprouts emerge from different axial vessels: first, the dorsal aorta, and then the posterior cardinal vein. In the case of the hindbrain, both sets of sprouts emerge from the same vessels, the PHBCs, although the direction of sprouting with respect to one another is perpendicular. Hindbrain CtAs and trunk ISVs both sprout and grow in a metamerically repeating pattern. In the case of trunk ISVs, the vessels form along the somite boundaries, whereas in the hindbrain the CtAs grow through the center of the rhombomeres, not along their boundaries.

In the trunk, vascular assembly and patterning are directed by a number of positive and negative cues. Vegfa expressed throughout the somites provides a pro-angiogenic cue that promotes dorsalward ISV sprouting and growth from the dorsal aorta. Type 3 semaphorins expressed in the central regions of the somites provide a repulsive signal for ISV endothelial cells, restricting their migration along the somite boundaries (Torres-Vazquez et al., 2004). Laminin matrix deposited along the intersomitic boundaries acts as an additional permissive cue, helping to promote ISV growth along intersomitic boundaries (Pollard et al., 2006). Our understanding of the cues that direct the assembly and patterning of the brain vasculature is more limited at this point. We have shown that VEGF signaling is required for both PHBC and BA formation. We have also shown that BA assembly requires ventral neural midline expression of chemokine ligands and endothelial expression of the chemokine receptor. Our data also suggest that chemokine-directed migration and alignment are mediated via the PI3K signaling pathway. Chemokine signaling does not appear to be absolutely required for angiogenic sprouting from the PHBC, as medial and dorsal waves of sprouting from the PHBC both still take place in animals injected with *cxc4a* MO or *cxc12b* MO. PHBC sprouting is inhibited in these animals, but recovers somewhat after a delay.

MO-injected animals do show a strong defect in endothelial cell migration from the PHBC and in the alignment of endothelial cells at the ventral neural keel to assemble a BA. A previous study reported that Cxcl12 gradients promote endothelial cell clustering, but that once endothelial cells contact each other Ephrin B2-EphB4 contributes to subsequent cell movement and alignment into cord-like structures (Salvucci et al., 2006). In the absence of proper chemokine signaling, one might therefore expect abnormal patterns of endothelial cell clustering, alignment and cord formation to arise as endothelial sprouts come into contact in aberrant ways. Indeed, we observe abnormal connections between PHBC-derived and LDA-derived sprouts in animals injected with *cxc4a* MO and/or *cxc12b* MO. As in other vertebrates, zebrafish LDAs normally only link indirectly to the BA via LDA-primitive internal carotid artery (PICA)-PCS-BA (Isogai et al., 2001). However, because the PHBC and LDA develop in reasonably close proximity to one another, misdirected sprouts from each of these vessels probably readily come into contact with endothelial cells from the other, then proceed to further alignment and lumenization, stabilizing abnormal connections. As noted above, the cranial CtAs also originate by sprouting from the PHBC, growing first dorsally, then medially, then ventrally to make connections to the BA. Although the BA does not generate any CtA sprouts itself, it serves as the target for PHBC-derived CtA connection, and this targeting is also disrupted in animals injected with *cxc4a* MO or *cxc12b* MO. However, as we have shown, it is not possible for us to determine whether CtA

defects reflect a direct requirement for chemokine signaling to target CTA sprouts to the BA, or an indirect consequence of improper BA formation and/or defects in some BA-derived targeting cue. Further studies will be required to dissect out these and other later functions of chemokine signaling in vascular development.

Acknowledgements

We thank Dr Igor Dawid for helpful discussions and members of the B.M.W. lab for technical help and critical suggestions. M.F. was supported by a fellowship from the Japan Society for the Promotion of Science (NIH). This research was supported by the intramural program of the NICHD, NIH (B.M.W.), by the Leducq Foundation (B.M.W.), and by the intramural program of the NIDCR (J.S.G.). Deposited in PMC for release after 12 months.

Competing interests statement

The authors declare no competing financial interests.

Supplementary material

Supplementary material for this article is available at <http://dev.biologists.org/lookup/suppl/doi:10.1242/dev.058776/-DC1>

References

- Busmann, J., Bakkers, J. and Schulte-Merker, S. (2007). Early endocardial morphogenesis requires *Scf/Tal1*. *PLoS Genet.* **3**, e140.
- Busmann, J., Wolfe, S. A. and Siekmann, A. F. (2011). Arterial-venous network formation during brain vascularization involves hemodynamic regulation of chemokine signaling. *Development* **138**, 1717-1726.
- Coffin, J. D. and Poole, T. J. (1988). Embryonic vascular development: immunohistochemical identification of the origin and subsequent morphogenesis of the major vessel primordia in quail embryos. *Development* **102**, 735-748.
- Coffin, J. D., Harrison, J., Schwartz, S. and Heimark, R. (1991). Angioblast differentiation and morphogenesis of the vascular endothelium in the mouse embryo. *Dev. Biol.* **148**, 51-62.
- Covassin, L., Amigo, J. D., Suzuki, K., Teplyuk, V., Straubhaar, J. and Lawson, N. D. (2006a). Global analysis of hematopoietic and vascular endothelial gene expression by tissue specific microarray profiling in zebrafish. *Dev. Biol.* **299**, 551-562.
- Covassin, L. D., Villefranc, J. A., Kacergis, M. C., Weinstein, B. M. and Lawson, N. D. (2006b). Distinct genetic interactions between multiple Vegf receptors are required for development of different blood vessel types in zebrafish. *Proc. Natl. Acad. Sci. USA* **103**, 6554-6559.
- DeRuiter, M. C., Poelmann, R. E., Mentink, M. M., Vaniperen, L. and Gittenberger-De Groot, A. C. (1993). Early formation of the vascular system in quail embryos. *Anat. Rec.* **235**, 261-274.
- Fouquet, B., Weinstein, B. M., Serluca, F. C. and Fishman, M. C. (1997). Vessel patterning in the embryo of the zebrafish: guidance by notochord. *Dev. Biol.* **183**, 37-48.
- Hong, C. C., Peterson, Q. P., Hong, J. Y. and Peterson, R. T. (2006). Artery/vein specification is governed by opposing phosphatidylinositol-3 kinase and MAP kinase/ERK signaling. *Curr. Biol.* **16**, 1366-1372.
- Isogai, S., Horiguchi, M. and Weinstein, B. M. (2001). The vascular anatomy of the developing zebrafish: an atlas of embryonic and early larval development. *Dev. Biol.* **230**, 278-301.
- Isogai, S., Lawson, N. D., Torrealday, S., Horiguchi, M. and Weinstein, B. M. (2003). Angiogenic network formation in the developing vertebrate trunk. *Development* **130**, 5281-5290.
- Jin, S. W., Herzog, W., Santoro, M. M., Mitchell, T. S., Frantsve, J., Jungblut, B., Beis, D., Scott, I. C., D'Amico, L. A., Ober, E. A. et al. (2007). A transgene-assisted genetic screen identifies essential regulators of vascular development in vertebrate embryos. *Dev. Biol.* **307**, 29-42.
- Jones, C. A. and Li, D. Y. (2007). Common cues regulate neural and vascular patterning. *Curr. Opin. Genet. Dev.* **17**, 332-336.
- Kamei, M. and Weinstein, B. M. (2005). Long-term time-lapse fluorescence imaging of developing zebrafish. *Zebrafish* **2**, 113-123.
- Kimmel, C. B., Ballard, W. W., Kimmel, S. R., Ullmann, B. and Schilling, T. F. (1995). Stages of embryonic development of the zebrafish. *Dev. Dyn.* **203**, 253-310.
- Knaut, H., Werz, C., Geisler, R. and Nusslein-Volhard, C. (2003). A zebrafish homologue of the chemokine receptor *Cxcr4* is a germ-cell guidance receptor. *Nature* **421**, 279-282.
- Kwan, K. M., Fujimoto, E., Grabher, C., Mangum, B. D., Hardy, M. E., Campbell, D. S., Parant, J. M., Yost, H. J., Kanki, J. P. and Chien, C. B. (2007). The Tol2kit: a multisite gateway-based construction kit for Tol2 transposon transgenesis constructs. *Dev. Dyn.* **236**, 3088-3099.
- Larson, J. D., Wadman, S. A., Chen, E., Kerley, L., Clark, K. J., Eide, M., Lippert, S., Nasevicius, A., Ekker, S. C., Hackett, P. B. et al. (2004). Expression of VE-cadherin in zebrafish embryos: a new tool to evaluate vascular development. *Dev. Dyn.* **231**, 204-213.
- Lawson, N. D. and Weinstein, B. M. (2002). In vivo imaging of embryonic vascular development using transgenic zebrafish. *Dev. Biol.* **248**, 307-318.
- Lawson, N. D., Scheer, N., Pham, V. N., Kim, C. H., Chitnis, A. B., Campos-Ortega, J. A. and Weinstein, B. M. (2001). Notch signaling is required for arterial-venous differentiation during embryonic vascular development. *Development* **128**, 3675-3683.
- Lawson, N. D., Vogel, A. M. and Weinstein, B. M. (2002). Sonic hedgehog and vascular endothelial growth factor act upstream of the Notch pathway during arterial endothelial differentiation. *Dev. Cell* **3**, 127-136.
- Lawson, N. D., Mugford, J. W., Diamond, B. A. and Weinstein, B. M. (2003). Phospholipase C gamma-1 is required downstream of vascular endothelial growth factor during arterial development. *Genes Dev.* **17**, 1346-1351.
- Lee, H. S., Han, J., Bai, H. J. and Kim, K. W. (2009). Brain angiogenesis in developmental and pathological processes: regulation, molecular and cellular communication at the neurovascular interface. *FEBS J.* **276**, 4622-4635.
- Leslie, J. D., Ariza-McNaughton, L., Bermange, A. L., McAdow, R., Johnson, S. L. and Lewis, J. (2007). Endothelial signalling by the Notch ligand Delta-like 4 restricts angiogenesis. *Development* **134**, 839-844.
- Matsuda, M. and Chitnis, A. B. (2009). Interaction with Notch determines endocytosis of specific Delta ligands in zebrafish neural tissue. *Development* **136**, 197-206.
- Nagasawa, T., Hirota, S., Tachibana, K., Takakura, N., Nishikawa, S., Kitamura, Y., Yoshida, N., Kikutani, H. and Kishimoto, T. (1996). Defects of B-cell lymphopoiesis and bone-marrow myelopoiesis in mice lacking the CXC chemokine PBSF/SDF-1. *Nature* **382**, 635-638.
- Olesnicki Killian, E. C., Birkholz, D. A. and Artinger, K. B. (2009). A role for chemokine signaling in neural crest cell migration and craniofacial development. *Dev. Biol.* **333**, 161-172.
- Padgett, D. H. (1956). The cranial venous system in man in reference to development, adult configuration, and relation to the arteries. *Am. J. Anat.* **98**, 307-355.
- Pham, V. N., Lawson, N. D., Mugford, J. W., Dye, L., Castranova, D., Lo, B. and Weinstein, B. M. (2007). Combinatorial function of ETS transcription factors in the developing vasculature. *Dev. Biol.* **303**, 772-783.
- Pickar, A., Scholpp, S., Bohl, H., Takeda, H. and Brand, M. (2002). A novel positive transcriptional feedback loop in midbrain-hindbrain boundary development is revealed through analysis of the zebrafish *pax2.1* promoter in transgenic lines. *Development* **129**, 3227-3239.
- Pollard, S. M., Parsons, M. J., Kamei, M., Kettleborough, R. N., Thomas, K. A., Pham, V. N., Bae, M. K., Scott, A., Weinstein, B. M. and Stemple, D. L. (2006). Essential and overlapping roles for laminin α chains in notochord and blood vessel formation. *Dev. Biol.* **289**, 64-76.
- Raz, E. and Mahabaleshwar, H. (2009). Chemokine signaling in embryonic cell migration: a fish eye view. *Development* **136**, 1223-1229.
- Roman, B. L., Pham, V. N., Lawson, N. D., Kulik, M., Childs, S., Lekven, A. C., Garrity, D. M., Moon, R. T., Fishman, M. C., Lechleider, R. J. et al. (2002). Disruption of *acvrl1* increases endothelial cell number in zebrafish cranial vessels. *Development* **129**, 3009-3019.
- Salvucci, O., de la Luz Sierra, M., Martina, J. A., McCormick, P. J. and Tosato, G. (2006). EphB2 and EphB4 receptors forward signaling promotes SDF-1-induced endothelial cell chemotaxis and branching remodeling. *Blood* **108**, 2914-2922.
- Sehnert, A. J., Huq, A., Weinstein, B. M., Walker, C., Fishman, M. and Stainier, D. Y. (2002). Cardiac troponin T is essential in sarcomere assembly and cardiac contractility. *Nat. Genet.* **31**, 106-110.
- Sepich, D. S., Ho, R. K. and Westerfield, M. (1994). Autonomous expression of the *nic1* acetylcholine receptor mutation in zebrafish muscle cells. *Dev. Biol.* **161**, 84-90.
- Sepich, D. S., Wegner, J., O'Shea, S. and Westerfield, M. (1998). An altered intron inhibits synthesis of the acetylcholine receptor α -subunit in the paralyzed zebrafish mutant *nic1*. *Genetics* **148**, 361-372.
- Siekmann, A. F. and Lawson, N. D. (2007). Notch signalling limits angiogenic cell behaviour in developing zebrafish arteries. *Nature* **445**, 781-784.
- Siekmann, A. F., Standley, C., Fogarty, K. E., Wolfe, S. A. and Lawson, N. D. (2009). Chemokine signaling guides regional patterning of the first embryonic artery. *Genes Dev.* **23**, 2272-2277.
- Swift, M. R. and Weinstein, B. M. (2009). Arterial-venous specification during development. *Circ. Res.* **104**, 576-588.
- Szymczak, A. L., Workman, C. J., Wang, Y., Vignali, K. M., Dilioglou, S., Vanin, E. F. and Vignali, D. A. (2004). Correction of multi-gene deficiency in vivo using a single 'self-cleaving' 2A peptide-based retroviral vector. *Nat. Biotechnol.* **22**, 589-594.
- Tachibana, K., Hirota, S., Iizasa, H., Yoshida, H., Kawabata, K., Kataoka, Y., Kitamura, Y., Matsushima, K., Yoshida, N., Nishikawa, S. et al. (1998). The chemokine receptor CXCR4 is essential for vascularization of the gastrointestinal tract. *Nature* **393**, 591-594.
- Thompson, M. A., Ransom, D. G., Pratt, S. J., MacLennan, H., Kieran, M. W., Detrich, H. W., 3rd, Vail, B., Huber, T. L., Paw, B., Brownlie, A. J. et al.

- (1998). The cloche and spadetail genes differentially affect hematopoiesis and vasculogenesis. *Dev. Biol.* **197**, 248-269.
- Torres-Vazquez, J., Gitler, A. D., Fraser, S. D., Berk, J. D., Van, N. P., Fishman, M. C., Childs, S., Epstein, J. A. and Weinstein, B. M.** (2004). Semaphorin-plexin signaling guides patterning of the developing vasculature. *Dev. Cell* **7**, 117-123.
- Villefranc, J. A., Amigo, J. and Lawson, N. D.** (2007). Gateway compatible vectors for analysis of gene function in the zebrafish. *Dev. Dyn.* **236**, 3077-3087.
- Viola, A. and Luster, A. D.** (2008). Chemokines and their receptors: drug targets in immunity and inflammation. *Annu. Rev. Pharmacol. Toxicol.* **48**, 171-197.
- Volin, M. V., Joseph, L., Shockley, M. S. and Davies, P. F.** (1998). Chemokine receptor CXCR4 expression in endothelium. *Biochem. Biophys. Res. Commun.* **242**, 46-53.
- Westerfield, M.** (2000). *The Zebrafish Book: A Guide for Laboratory Use of Zebrafish (Danio rerio)*. Eugene, OR: University of Oregon Press.
- Williams, C., Kim, S. H., Ni, T. T., Mitchell, L., Ro, H., Penn, J. S., Baldwin, S. H., Solnica-Krezel, L. and Zhong, T. P.** (2010). Hedgehog signaling induces arterial endothelial cell formation by repressing venous cell fate. *Dev. Biol.* **341**, 196-204.
- Wilson, B. D., Li, M., Park, K. W., Suli, A., Sorensen, L. K., Larrieu-Lahargue, F., Urness, L. D., Suh, W., Asai, J., Kock, G. A. et al.** (2006). Netrins promote developmental and therapeutic angiogenesis. *Science* **313**, 640-644.
- Zannino, D. A. and Appel, B.** (2009). Olig2+ precursors produce abducens motor neurons and oligodendrocytes in the zebrafish hindbrain. *J. Neurosci.* **29**, 2322-2333.
- Zheng, H., Fu, G., Dai, T. and Huang, H.** (2007). Migration of endothelial progenitor cells mediated by stromal cell-derived factor-1 α /CXCR4 via PI3K/Akt/eNOS signal transduction pathway. *J. Cardiovasc. Pharmacol.* **50**, 274-280.
- Zhong, T. P., Rosenberg, M., Mohideen, M. A., Weinstein, B. and Fishman, M. C.** (2000). *gridlock*, an HLH gene required for assembly of the aorta in zebrafish. *Science* **287**, 1820-1824.
- Zhong, T. P., Childs, S., Leu, J. P. and Fishman, M. C.** (2001). Gridlock signalling pathway fashions the first embryonic artery. *Nature* **414**, 216-220.